ADVANCED FUNCTIONAL MATERIALS
www.afm-journal.de

Multifunctional Modification of SIS Membrane with Chimeric Peptides to Promote Its Antibacterial, Osteogenic, and Healing-Promoting Abilities for Applying to GBR

Yuzhu Mu, Shiqing Ma, Pengfei Wei, Yonglan Wang, Wei Jing, Yifan Zhao, Lei Zhang, Jinzhe Wu, Bo Zhao, Jiayin Deng,* and Zihao Liu**

Guided bone regeneration (GBR) technology is the most widely used and stable method for bone defect repair. However, infectious bone defect limits the application of this technique. Herein, a small intestinal submucosa (SIS) membrane modified by chimeric peptides as a new type of GBR membrane is developed for efficacious tissue regeneration. Based on the main components of SIS membrane are I and III collagen, collagen binding peptides TKKTLRT and KELNLVY sequences are used to construct chimeric peptides with healing-promoting peptide Hst1 or antibacterial osteogenic peptide JH8194, so as to realize the specifically target of SIS. This method achieves the fast and efficient multifunctional modification of SIS membrane. The chimeric peptides modified SIS (pSIS) membrane has satisfactory biocompatibility and a certain degree of antibacterial activity. Moreover, pSIS promotes the osteogenic related factors expression of rat bone mesenchymal stem cells and demonstrates great bone regeneration in rat skull defect model. Furthermore, pSIS accelerates the migration of oral epithelial cells in vitro and activate integrin $\alpha 3\beta 1$ signal pathway contribute to wound healing. This study presents a novel biomaterial design of GBR membrane, specifically for the treatment of infectious bone defects.

1. Introduction

Bone defect caused by trauma, tumor, inflammation, and other reasons remain as irremediable obstacles in current bone reconstruction. Periodontitis and peri-implantitis are common causes of alveolar bone loss due to plaque biofilm, which can eventually lead to tooth or implant loss and insufficient bone of dental implant area. Guided bone regeneration (GBR) technology is considered as one of the methods most commonly applied to reconstruct bone deficiencies.[1] It requires a barrier membrane to prevent the growth of epithelial cells and fibrous connective tissue into defect area, thus ensuring osteoblasts can fill the bone defect space to obtain the desired bone regeneration.[2] The performance of GBR membrane plays an important role in the application of GBR technology, which is closely related to the prevention of bacterial infection, wound healing and bone regeneration after GBR operation.

Extracellular matrix (ECM) material is a noncellular biological network composed of collagen (mainly type I and III) and various proteins, which has become a hotspot for tissue engineering scaffold in recent years.[3] Small intestinal submucosa (SIS) is the most commonly used ECM material because of its wide sources and easy availability. SIS has many excellent properties, including site-specific tissue regeneration ability, low immunogenicity, excellent mechanical properties, as well as contains multifarious cytokines.[4] It has been used as scaffold material in many types of tissue and achieved satisfactory results.[5] However, infectious bone defect caused by periodontitis, peri-implantitis, and periapical periodontitis is a difficult problem for GBR.[6] Although SIS membrane has excellent mechanical properties and biocompatibility, its antibacterial, osteogenic, and healing-promoting properties are limited.[7] To address these limitations, we hope to find a suitable way for modification of SIS.

Antimicrobial peptides (AMPs), as an important part of innate immunity, show broad spectrum, strong and stable antimicrobial activities and great biocompatibility, having become a new generation of potential antibacterial drugs.[8] Histatins (Hsts) are a class of AMPs secreted by human main salivary glands. Due to the cation and weak amphiphilic character, Hsts exhibit broad-spectrum antibacterial activity in warm and humid oral environment.[9] Hst5 is a major member of Hsts, which can resist lipopolysaccharide (LPS) of *Porphyromonas gingivalis* (Pg) by inhibitor of nuclear factor kappa-B kinase (IKK)/nuclear factor kappa-B (NF-κB) pathway and inhibit the expression of interleukin (IL)-6 and IL-8 induced by *Pg* outer

Y. Mu, Dr. S. Ma, Prof. Y. Wang, Y. Zhao, L. Zhang, J. Wu, Prof. J. Deng, Dr. Z. Liu
School and Hospital of Stomatology
Tianjin Medical University
12 Observatory Road, Tianjin 30070, China
E-mail: jdeng@tmu.edu.cn; liuzihao@tmu.edu.cn
Dr. P. Wei, Dr. W. Jing, Prof. B. Zhao
Beijing Biosis Healing Biological Technology Co., Ltd.
No. 6 Plant West, Valley No. 1 Bio-medicine Industry Park, Beijing 102600, China
E-mail: zhaobo@biosishealing.com
The ORCID identification number(s) for the author(s) of this article can be found under https://doi.org/10.1002/adfm.202101452.

DOI: 10.1002/adfm.202101452

membrane protein.[10] Our previous study has showed that JH8194, a derivative peptide of Hst5, also has good antibacterial activity which can prevent peri-implantitis and peri-implant mucositis effectively.[11] Except for antibacterial activity, JH8194 also has a certain ability to promote bone formation. It has been found that JH8194 could stimulate the expressions of runt-related transcription factor 2 (Runx2), osteopontin (Opn), and alkaline phosphatase (Alp) in MC3T3-E1 while inhibiting the biofilm formation of *Pg*, so that the cells can differentiate into osteoblasts.[12] Additionally, JH8194 can increase the formation of mature trabecular bone around the implant and enhance the osseointegration, which is conducive to the long-term stability of the implant.[13] Therefore, JH8194 is an effective drug for antibacterial and osteogenic modification of SIS membrane.

Surprisingly, Hst1, another member of HSTs, has shown superior ability in healing-promoting. Hst1 could promote the migration or adhesion of fibroblasts, epithelial cells, and endothelial cells, as well as guide re-epithelialization and vascular regeneration of the wound area.[14] The mechanism by which Hst1 enhances wound healing is still not completely understood. Some studies find that Hst1 binds to G protein-coupled receptors (GPCR) and activates G protein, which subsequently activates downstream unknown kinases and induces extracellular signal-regulated kinases (ERK1/2)/mitogen-activated protein (MAP) phosphorylation, eventually promotes cell spreading, migration, and adhesion.[14a,15] Thus, loading Hst1 may enhance the healing-promoting function of SIS on the basis of JH8194, but the specific mechanism still needs to be explored.

Despite these advantages, how to bind peptides to SIS membrane is still a challenge. In recent years, chimeric peptide, a kind of small peptide protein constructed by connecting two or more functional polypeptide molecules, has shown tremendous potentiality in drug delivery.[16] Considering the characteristics of SIS membrane with type I and III collagen as the main component, collagen binding peptides are chosen. TKKTLRT derived from collagenase has a strong affinity with type I collagen due to high ratio of polar amino acids to nonpolar amino acids. It has been combined with a variety of growth factors or drug fragments successfully and delivered them to type I collagen.[17] In addition, KELNLVY derived from platelet can bind to type III collagen specifically.[18] Using TKKTLRT and KELNLVY sequences to construct chimeric peptides with Hst1 and JH8194 is expected to achieve peptides loading specifically of SIS membrane (**Figure 1**A). The chimeric peptides are composed of three parts, collagen binding peptides (type I collagen: TKKTLRT or type III collagen: KELNLVY), functional peptides (Hst1 or JH8194), and a flexible linker (GGGGSGGGGS). The multifunctional modification of SIS membrane with chimeric peptides can improve antibacterial, osteogenic, and healing-promoting abilities of SIS and provide a new direction for the development of GBR membranes.

2. Results and Discussion

2.1. Design of Chimeric Peptides Modified SIS (pSIS) Membrane

The design details of pSIS membrane and structure prediction of chimeric peptides are shown in Figure 1. The four chimeric peptides were composed of collagen binding peptides (TKKTLRT or KELNLVY), functional peptides (Hst1 or JH8194), and a flexible linker (GGGGSGGGGS). "GGGGS" is the most commonly used flexible linker consisting of glycine (Gly) and serine (Ser) residues,[19] which can ensure the flexibility and mobility of connecting functional domains. In this study, copy number 2 was used to achieve appropriate separation of the functional domains and avoid mutual interference.[20] The prediction results showed that P1-4 had one or several basic structures, such as α-helix, β-sheet, and random coils, and their spatial structures were different (Figure 1B).

2.2. Binding and Release Abilities of Chimeric Peptides on the Surface of SIS Membrane

Subsequently, the SIS membranes were soaked in different concentrations of P1, P2, P3, and P4 solutions to observe the binding ability of chimeric peptides on the surface by confocal laser scanning microscopy (CLSM). As the concentration increased from 50 to 200×10^{-6} M, the fluorescent label on the SIS membrane increased, which meant that more chimeric peptides were bound (**Figure 2**A). In particular, after soaking with 200×10^{-6} M chimeric peptides solutions, more than 85% fluorescent area of the SIS membrane (H-pSIS) realized the effective binding. Previous research showed that the SIS membrane used in this study contained 28.09 ± 0.67% type I collagen and 59.50 ± 1.42% type III collagen.[21] To further determine the maximum binding capacity, the concentration of chimeric peptide solutions was increased to 400×10^{-6} M (Figure S1, Supporting Information). The result was similar to 200×10^{-6} M, and the binding amount of P1/P2 and P3/P4 did not increase, indicating that the binding capacity of four chimeric peptides reached the maximum at 200×10^{-6} M. Although the ratio of type I and type III collagen was about 1:2, the binding amount of P1/P2 bound to type I collagen and P3/P4 bound to type III collagen was nearly similar (Figure 2A and Figure S1, Supporting Information), which might be because the binding ability of TKKTLRT to type I collagen was stronger than that of KELNLVY to type III collagen.

Then, the SIS membranes soaked in 50×10^{-6} M (L-pSIS), 100×10^{-6} M (M-pSIS), and 200×10^{-6} M (H-pSIS) were selected to observe the surface morphology by scanning electron microscopy (SEM) (Figure 2B). Compared with SIS, pSIS still maintained a similar structure and had small particle-like substances formed by specific combination of a large number of chimeric peptides with SIS membrane. Lyophilization process did not affect the structure of the SIS membrane and the stable binding of chimeric peptides. The higher the concentration of chimeric peptides solution, the more particles on the surface of pSIS. However, because of the minuscule molecular weight of chimeric peptides, SEM could only observe a large number of aggregated particles, which might not match the binding rate observed under CLSM. Moreover, the cross-section of SIS was observed by SEM (Figure S2, Supporting Information), and it could be seen that SIS had a certain thickness, about 300–350 μm, which was important for SIS and pSIS membrane to play the role of supporting and barrier in bone defect area.

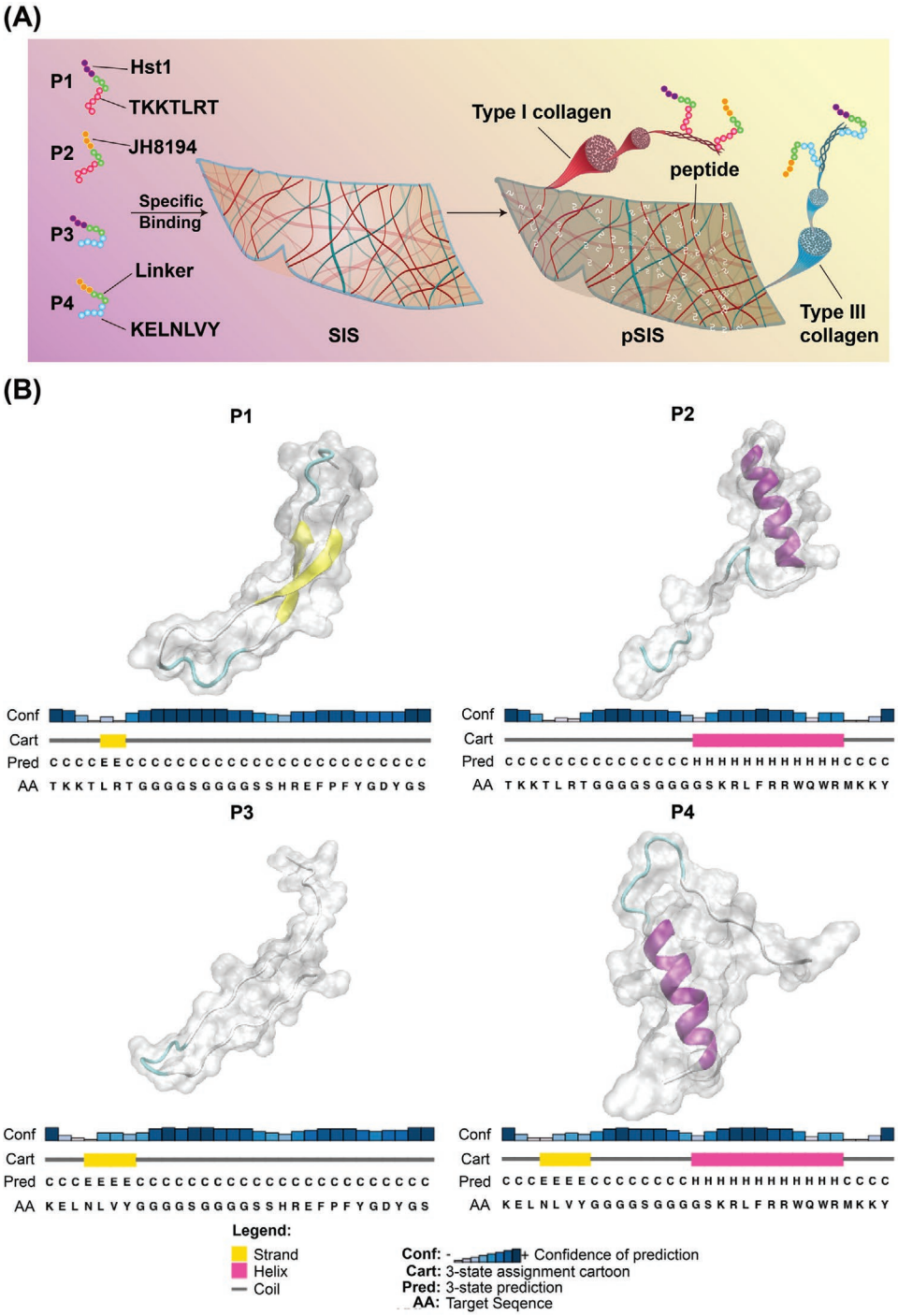

Figure 1. Design of pSIS membrane and structure prediction of chimeric peptides. A) Schematic of pSIS membrane. The chimeric peptides consist of three parts: P1 and P2: TKKTLRT (binds to type I collagen of SIS membrane), Hst1/JH8194 (plays antibacterial, osteogenic, and healing-promoting ability functions), and GGGGSGGGGS (connects these first two parts), P3 and P4: KELNLVY (binds to type III collagen of SIS membrane), Hst1/JH8194 and GGGGSGGGGS. B) Secondary structure and 3D views of chimeric peptides.

To further clarify the release of chimeric peptides, taking H-pSIS group as an example, we observed the binding number of chimeric peptides on the pSIS membrane by CLSM after 1, 3, and 7 d of cell culture (Figure 2C). On the first day, a large number of chimeric peptides could be observed on the H-pSIS membrane. With the extension of time, the chimeric peptides bound on the surface of H-pSIS membrane decreased. This trend may be due to the degradation of chimeric peptides caused by enzymes in the microenvironment, and the protein crown may compete for the binding sites and replace the chimeric

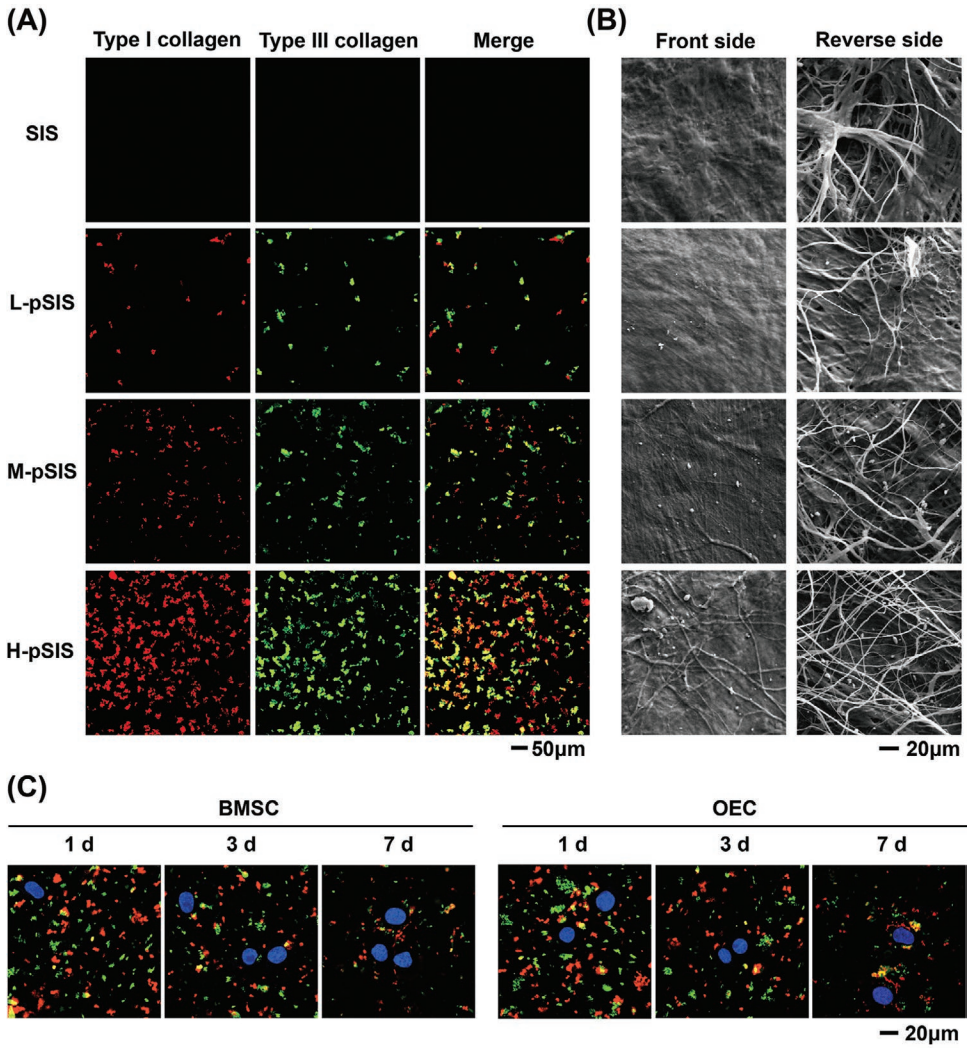

Figure 2. Binding and release abilities of chimeric peptides on the surface of SIS membrane. A) CLSM observed the binding ability of chimeric peptides. (SIS: soaked in PBS, L-pSIS: soaked in four chimeric peptides solutions of 50×10^{-6} M, M-pSIS: soaked in four chimeric peptides solutions of 100×10^{-6} M, H-pSIS: soaked in four chimeric peptides solutions of 200×10^{-6} M.) B) The surface morphology of freeze-drying SIS and pSIS membranes were observed by SEM. C) Release of chimeric peptides on the pSIS membrane observed by CLSM (nucleus: blue).

peptides on the surface of pSIS membrane.[16] After 7 d, the content of chimeric peptides decreased significantly, but it still could be observed on H-pSIS membrane, indicating chimeric peptides could maintain for a certain time and release continuously to the surrounding environment. In addition, some chimeric peptides were closely distributed around the cells on the seventh day, which might play a biological role in the cells.

2.3. Biocompatibility of pSIS In Vitro

Biocompatibility, the interaction among material and host, is a fundamental characteristic of materials to ensure the safety of patients during application.[22] The effect of pSIS on cell proliferation was explored by carboxyfluorescein succinimidyl ester (CFSE) staining and CCK-8. CFSE staining on the fourth cell culturing day was analyzed by flow cytometry (**Figure 3**A). It was found that the proliferation ability of BMSCs and OECs in SIS and pSIS groups was higher than the control group, which might be related to a variety of cytokines contained in SIS, such as endothelial growth factor (EGF) and vascular endothelial growth factor (VEGF).[4a] However, the values of SIS and pSIS groups were close, indicating that chimeric peptides could not promote proliferation of BMSCs and OECs which is related to bone reconstruction and soft tissue healing during GBR. This was consistent with the results of other studies,[12,14b,15b] suggesting that the promotion of cell proliferation was not the main function and mechanism of pSIS in the application of GBR. Furthermore, it showed that BMSCs and OECs of each group proliferated logarithmically in CCK-8 assay (Figure 3B). On the second day, the proliferation ability of BMSCs on H-pSIS membrane was lower than other groups significantly, but with the time prolongation, the proliferation ability increased and there was no statistical difference with other groups. The proliferation ability of BMSCs and OECs reached the platform stage on the sixth day. These results showed that

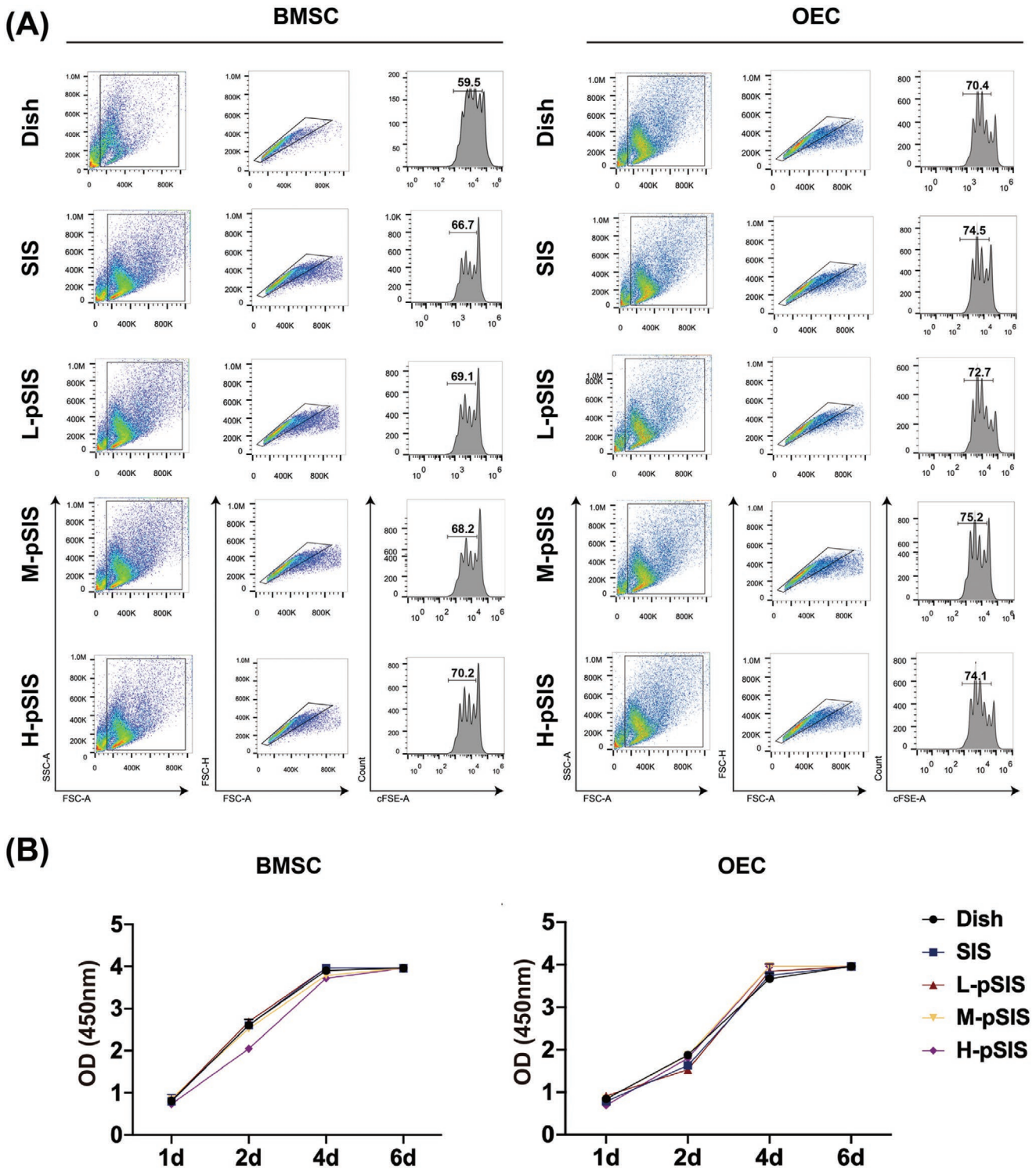

Figure 3. Biocompatibility of pSIS in vitro. A) CFSE cell proliferation assay by flow cytometry of BMSCs and OECs on the fourth day. B) Proliferation ability of BMSCs and OECs by CCK-8.

pSIS had no obvious cytotoxicity. The robust biocompatibility was helpful for the application of pSIS in GBR. Taken the above results into consideration, we selected M-pSIS and H-pSIS with higher binding rate of chimeric peptides for further exploration in the subsequent experiments.

2.4. Antibacterial Activity of pSIS In Vitro

To investigate the antibacterial activity of pSIS against *Streptococcus sanguis* (*S. sanguis*) and *Streptococcus gordonii* (*S. gordonii*), inhibitory rings and CLSM were detected (**Figure 4**). Although

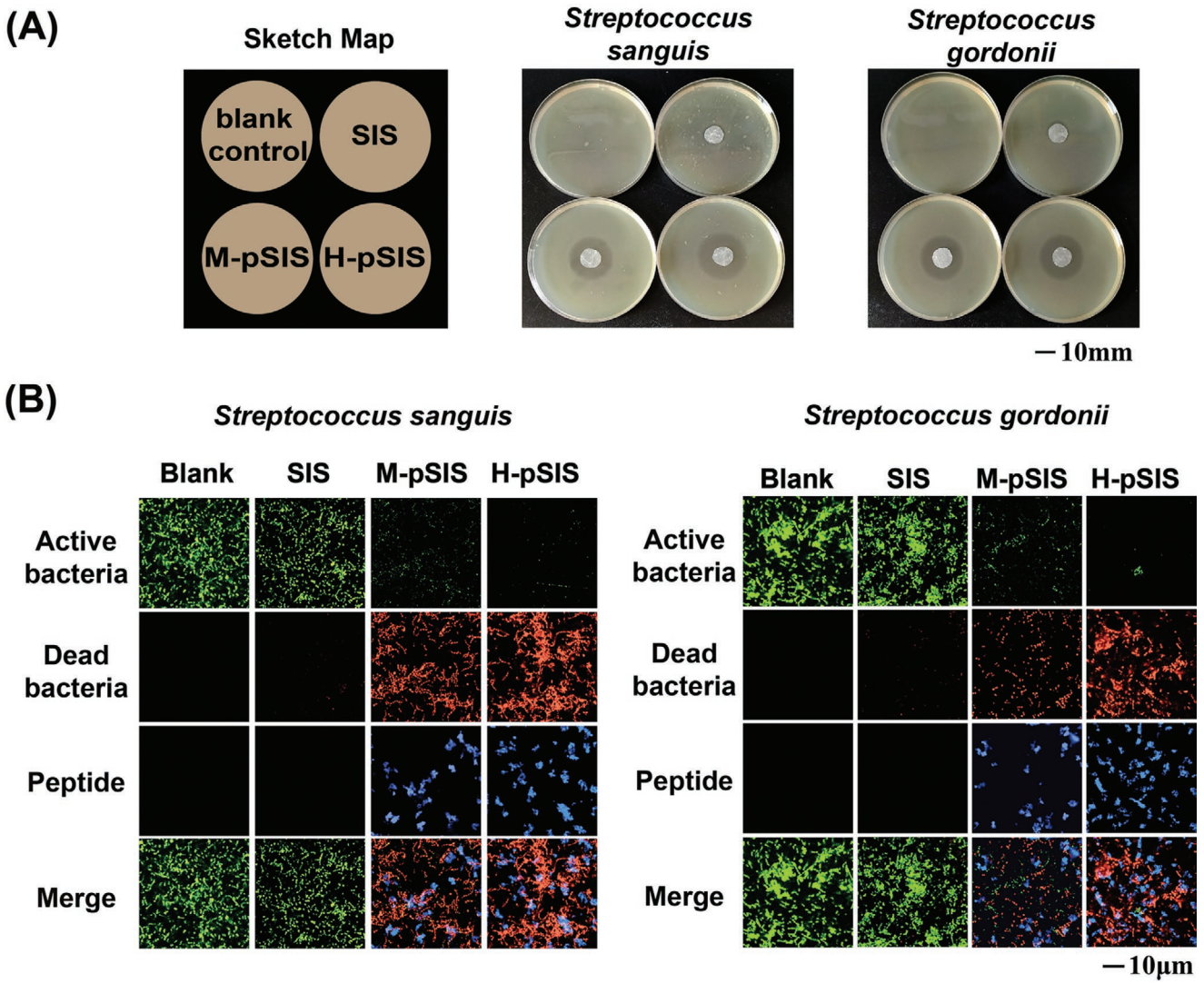

Figure 4. Antibacterial activity of pSIS in vitro. A) Inhibitory rings of *S. sanguis* and *S. gordonii* (upper left: blank control, upper right: SIS, lower left: M-pSIS, lower right: H-pSIS). B) CLSM images of live/dead staining (live bacteria: green, dead bacteria: red, peptides: blue).

SIS could produce tiny inhibitory rings, the results were not statistically significant, while M-pSIS and H-pSIS could produce obvious inhibitory rings for two kinds of bacteria (Figure 4A). Additionally, the CLSM images show the live (green)/dead (red) colonies of bacteria (Figure 4B). Compared with the blank well, the SIS group had a small number of dead bacteria. Conversely, with the increase of peptide concentration (blue), dead bacteria of M-pSIS and H-pSIS increased sequentially, indicating that chimeric peptides enhanced the antibacterial activity of SIS membrane and H-pSIS was the strongest.

Plaque biofilms are multispecies microbial communities which can enhance the resistance of bacteria to host defense system and antimicrobial agents, finally leading to inflammation.[23] *S. gordonii* and *S. sanguis* are early colonizing bacteria of dental plaque biofilm.[24] Timely and early control of the above flora colonization will be conducive to the prevention of oral infection and inflammation after GBR operation. JH8194 is a derivative peptide of oral antimicrobial peptide Hst5. It has been found that AMPs and its derivatives could exchange divalent cations (e.g., Mg^{2+} and Ca^{2+}) on the bacterial membrane via an "ion-exchange mechanism" to disrupt the stability of cytoplasmic membrane, leading to cell death.[25] Moreover, the positively charged AMPs can adsorb on the negatively charged cytoplasmic membrane through electrostatic interaction and insert into phospholipid bimolecular layer to form pores or even larger defect on the membrane, eventually resulting in cytoplasmic leakage and bacterial death.[25]

2.5. Effect of pSIS on Osteogenic-Related Factors Expression of BMSCs

Osteogenesis is the key of GBR technology. The effect of pSIS on the expression of osteogenic-related factors of BMSCs was also assessed (**Figure 5**). Bone morphogenetic protein-2 (BMP2), RUNX2, ALP, and OPN are classical osteogenic factors.[26] As shown in Figure 5A, the mRNA levels of above osteogenic factors of pSIS groups were significantly higher

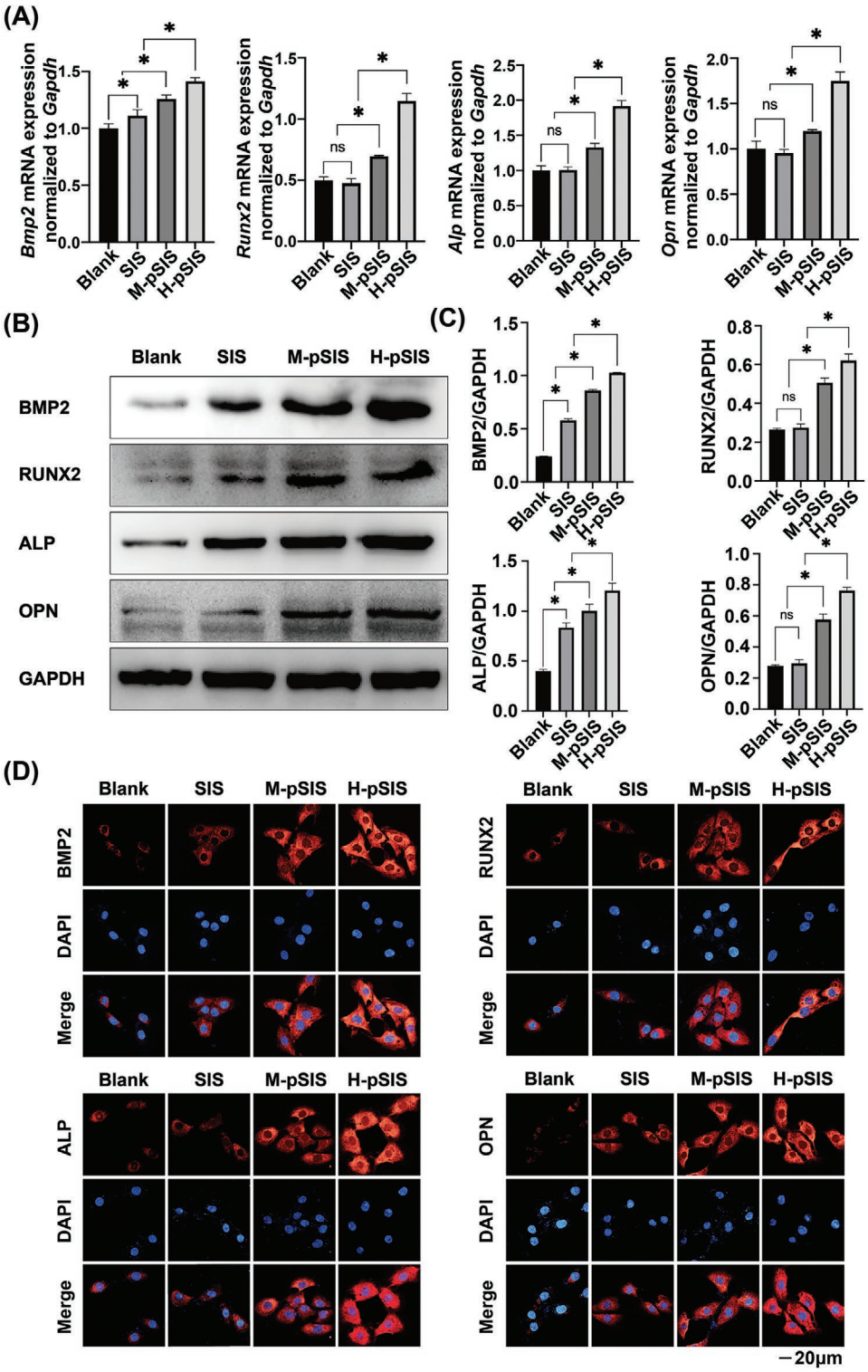

Figure 5. Effect of pSIS on osteogenic-related factors expression of BMSCs. A) qRT-PCR analysis of osteogenic-related genes (* represents $p < 0.05$). B) Western blot analysis of osteogenic-related proteins. C) Quantitative analysis of Western blot analysis (* represents $p < 0.05$). D) Immunofluorescence analysis of osteogenic-related proteins localizations in BMSCs (osteogenic-related proteins: red, nucleus: blue).

than blank control and SIS, and this trend was confirmed by Western blot analysis (Figure 5B,C). Then, the localization of BMP2, RUNX2, ALP, and OPN in cells was determined by CLSM (Figure 5D). It could be seen that the red fluorescence of M-pSIS and H-pSIS was significantly higher than that of SIS, and H-pSIS expressed the most fluorescent signals. The

proteins were distributed in cytoplasm far away from cell membrane. The above results indicated that pSIS membrane could promote the expression of osteogenic-related factors. Makihira et al. have found that JH8194 could enhance the expressions of *Runx2*, *Opn*, and ALPase activity in MC3T3-E1 and make cells differentiate into osteoblasts.[12] Thus, JH8194 might play an important role in the result that pSIS membrane promoted the expression of osteogenic-related factors.

2.6. Effects of pSIS on Cell Migration and Possible Signal Pathway of OECs

Wound healing process in GBR involves cell proliferation and migration, wound contraction and angiogenesis, collagen deposition and remodeling. Cell migration composed of multistep processes is necessary for wound repair.[27] Sequence "SHREFPFYGDYGS" of Hst1 contains the minimal elements necessary to promote cell migration, which can promote the migration of oral keratinocytes, oral epithelial cells, and gingival fibroblasts.[28] The effect of pSIS on migration of OECs was detected by Transwell experiments (**Figure 6**A,B). SIS and pSIS could promote the migration of OECs in which H-pSIS had the strongest ability, suggesting that chimeric peptides modified SIS membrane could promote cell migration furtherly and might contribute to the healing of soft tissue. In addition, we used the same method to explore the effect of pSIS on the migration of BMSCs (Figure S3, Supporting Information). The result was similar to that of OECs. SIS and pSIS, especially H-pSIS, could significantly promote the migration of BMSCs, which was helpful for the migration of BMSCs to the bone defect area to induce osteogenesis.

Subsequently, to explore the specific mechanism of chimeric peptides promoting OECs migration, RNA-seq, a novel high-throughput sequencing method, was used to analyze the differentially expressed genes of OECs cultured on SIS, M-pSIS, and H-pSIS membrane for 24 h (Figure 6C). Compared with the SIS group, there were 790 genes increased and 833 genes decreased in M-pSIS group, 756 genes increased and 735 genes decreased in H-pSIS group. Venn diagram showed that 844 genes had identical tendency. By clustering analysis of the different genes, we found that integrin-β1(ITG-β1) was related to cell migration (Figure 6D).

However, most integrin are heterodimeric molecules formed by the subunits α and β in a noncovalent connection, which mediates adhesion and migration of cells and plays an essential role in wound repair.[29] Integrin $\alpha3\beta1$ is closely related to cell migration and wound healing. It can promote re-epithelialization by accelerating migration of keratinocytes to assist the healing of epithelial wounds.[30] In the GBR region, integrin $\alpha3\beta1$ can bind to unprocessed laminin-5, then mediating the migration of connected epithelial cells.[31] Therefore, the expression of integrin-$\alpha3$ (ITG-$\alpha3$) and ITG-$\beta1$ of OECs was detected. The expression of ITG-$\alpha3$ and ITG-$\beta1$ in H-pSIS group was higher than SIS group (Figure 6E–G), showing that chimeric peptides could promote the expression of migration-related factors. Then, the localization of ITG-$\alpha3$ and ITG-$\beta1$ (red) in the cells was determined by CLSM (Figure 6H). It could be seen that the red fluorescence in H-pSIS group was stronger than SIS group, and the proteins were distributed in cytoplasm far away from cell membrane.

2.7. Evaluation of Osteogenic Ability of pSIS in Rat Skull Defect Model

In animal experiments, we selected the H-pSIS membrane with the best effect for in vivo study (**Figure 7**). The critical size defect (CSD) model of 8 mm round defect which could not self-heal was made in the rat to evaluate bone regeneration.[32] Moreover, Bio-Gide membrane, developed particularly for improving the ossification of bone defects of any origin in GBR,[33] was used as a control. As shown in Figure 7A, the micro-computed tomography (CT) images of all groups showed that the formation of new bone developed from the defect edge to the center. Twelve weeks after surgery, bone volume/total volume (BV/TV) of SIS group and Bio-Gide group was higher than blank control, but there was no significant difference between SIS and Bio-Gide. Moreover, H-pSIS group demonstrated greatly improved osteogenesis in vivo (Figure 7A,B).

Histological analysis was carried out by hematoxylin and eosin (H&E) and Masson's trichrome staining to evaluate growth of collagen and new bone tissue as well as the infiltration of lymphocytes. Collagen is an important component of bone. Osteoblast-secreted ECM including type I collagen may transform from amorphous and noncrystalline initially to more crystalline gradually leading to promote osteogenesis.[34] In addition, mineralization is a major process for osteoblasts to promote bone formation. Collagen serves as a template and may also initiate and propagate mineralization.[34] Therefore, collagen content is closely related to bone formation. As shown in Figure 7C,D, the defect area of blank control was mainly composed of fibrous tissue with less collagen, there was no obvious signs of new bone formation. However, the bone defect areas of SIS group, Bio-Gide group, and H-pSIS group were rich in collagen, and new bone was formed around the stump with small numbers of even none fibrous connective tissue invasion. Meanwhile, the lymphocyte infiltration of all groups was low, indicating that there was no inflammatory reaction (Figure 7C). The expression of osteocalcin (OCN) and collagen type 1 (COL1) was detected by immunohistochemistry (Figure 7E). Twelve weeks after surgery, the control group did not have obvious OCN and COL1 staining while they were highly expressed in the SIS, Bio-Gide, and H-pSIS groups, the H-pSIS group was the highest.

The above results showed that H-pSIS could effectively prevent the fibrous connective tissue from growing into the defect area, providing space for bone formation. The excellent bone regeneration capability of pSIS is helpful to solve the problems of alveolar bone loss caused by periodontitis or tooth loss and insufficient bone mass in the dental implant area. In addition, its unique anti-infective capability conduces to repair infective bone defects with resisting and preventing tissue inflammation and infection, which is expected to solve the clinical difficulty in repairing bone defects associated with infection.

2.8. Evaluation of Healing-Promoting Ability of pSIS in Rat Skin Defect Model

A rat skin defect model was constructed to evaluate the healing-promoting ability of pSIS. One and two weeks after

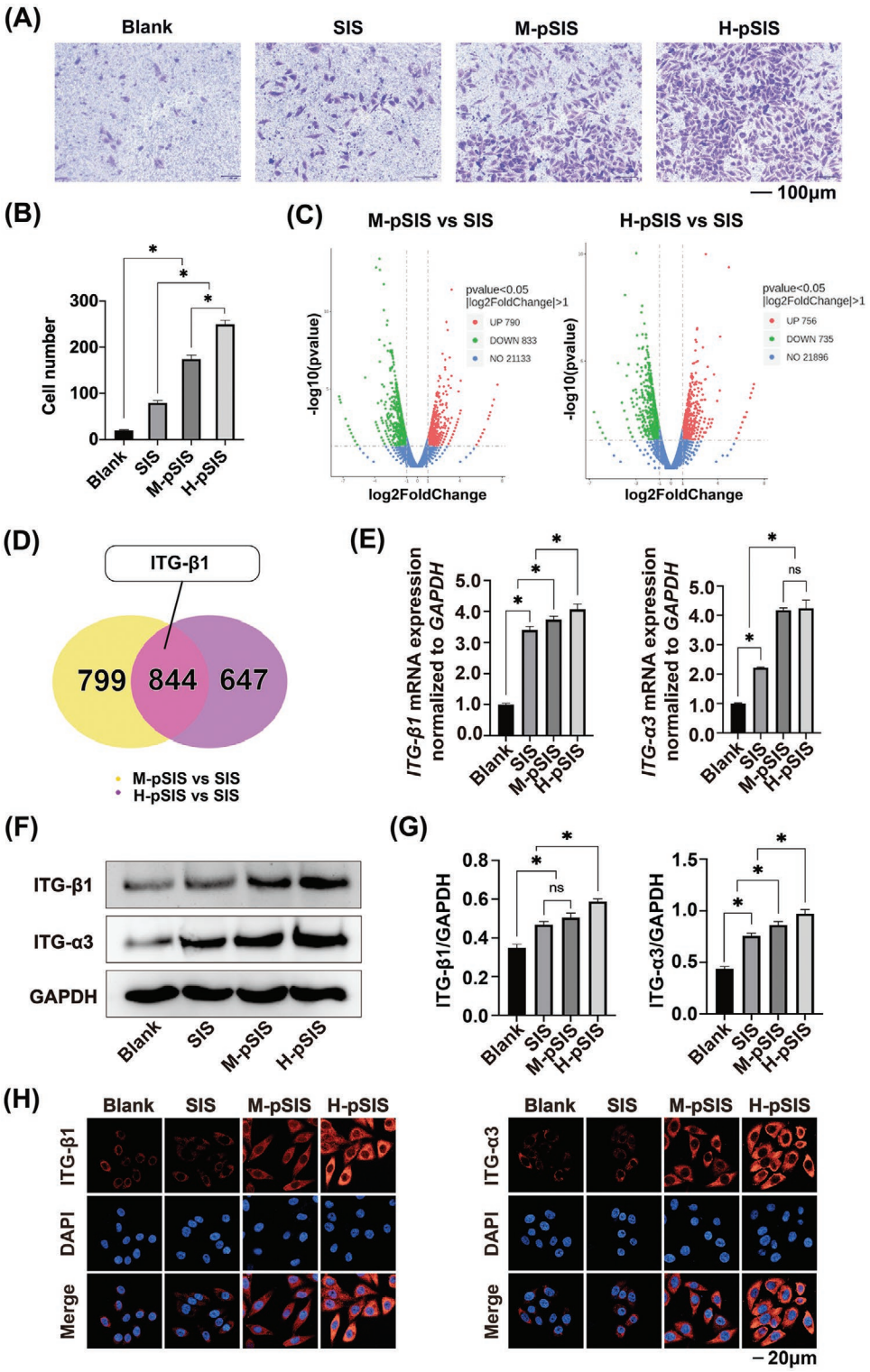

Figure 6. Effects of pSIS on OECs migration and its signal pathway. A) Transwell experiments to detect capability of OECs migration. B) Analysis of migrating cells (* represents $p < 0.05$). C) RNA-seq screened differentially expressed genes. D) Venn diagram of different genes. E) qRT-PCR analysis of migration-related genes. F) Western blot analysis of migration-related proteins. G) Quantitative analysis of Western blot analysis (* represents $p < 0.05$). H) Immunofluorescence analysis of migration-related proteins localizations in OECs (ITG-α3 and ITG-β1: red, nucleus: blue).

surgery, the healing effects of Bio-Gide, SIS, and H-pSIS were better than the blank control under direct vision (Figure S4, Supporting Information). Among them, H-pSIS had the best healing-promoting ability. Compared with

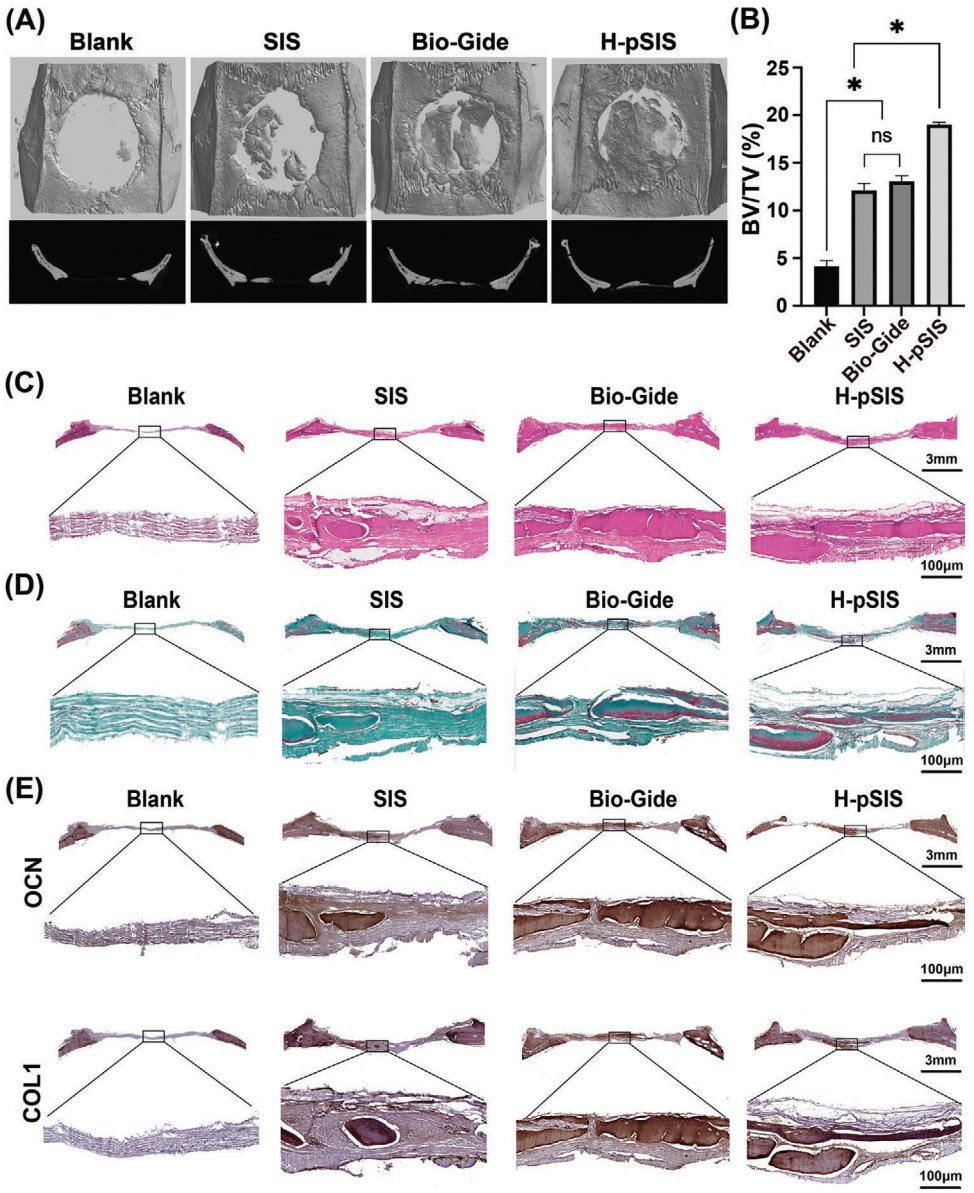

Figure 7. Evaluation of osteogenic ability of pSIS in rat skull defect model at 12 weeks. A) 3D reconstruction and sagittal image of bone defects covered with SIS, Bio-Gide, and H-pSIS membrane. B) BV/TV of bone defects in different groups (* represents $p < 0.05$). C) H&E staining. D) Masson's trichrome staining. E) Immunohistochemical analysis of OCN and COL1 expression.

other groups, the wound in this group was the smallest at one week and completely healing at two weeks. To evaluate the re-epithelialization and collagen content in the soft tissue defect area, histological analysis was carried out by H&E and Masson's trichrome staining (**Figure 8**A–D). As shown in Figure 8A,B, one and two weeks after surgery, the degree of re-epithelialization of SIS group and H-pSIS group was significantly higher than Bio-Gide and blank control, the H-pSIS was the highest. Re-epithelialization is a basic feature of wound healing, which is related to the directional migration of keratinocytes.[35] The pSIS membrane may accelerate the re-epithelialization through the promotion of cell migration, which is helpful for the rapid healing of wound. As with bone formation, the successful healing of wounds requires the local synthesis of a large amount of collagen.[36] The collagen content in the soft tissue defect area of H-pSIS was significantly higher than other groups (Figure 8C,D). It showed that H-pSIS had better ability of promoting soft tissue healing. The expression of ITG-α3 and ITG-β1 was detected by immunohistochemistry, the positive area was described in Figure 8E. A higher level of ITG-α3 and ITG-β1 in the SIS, Bio-Gide, and H-pSIS groups than control group, and the H-pSIS group was the highest. These results suggested that the chimeric peptides modified SIS membrane promoted epithelial cell migration and collagen deposition, which might be related to the increased expression of ITG-α3 and ITG-β1.

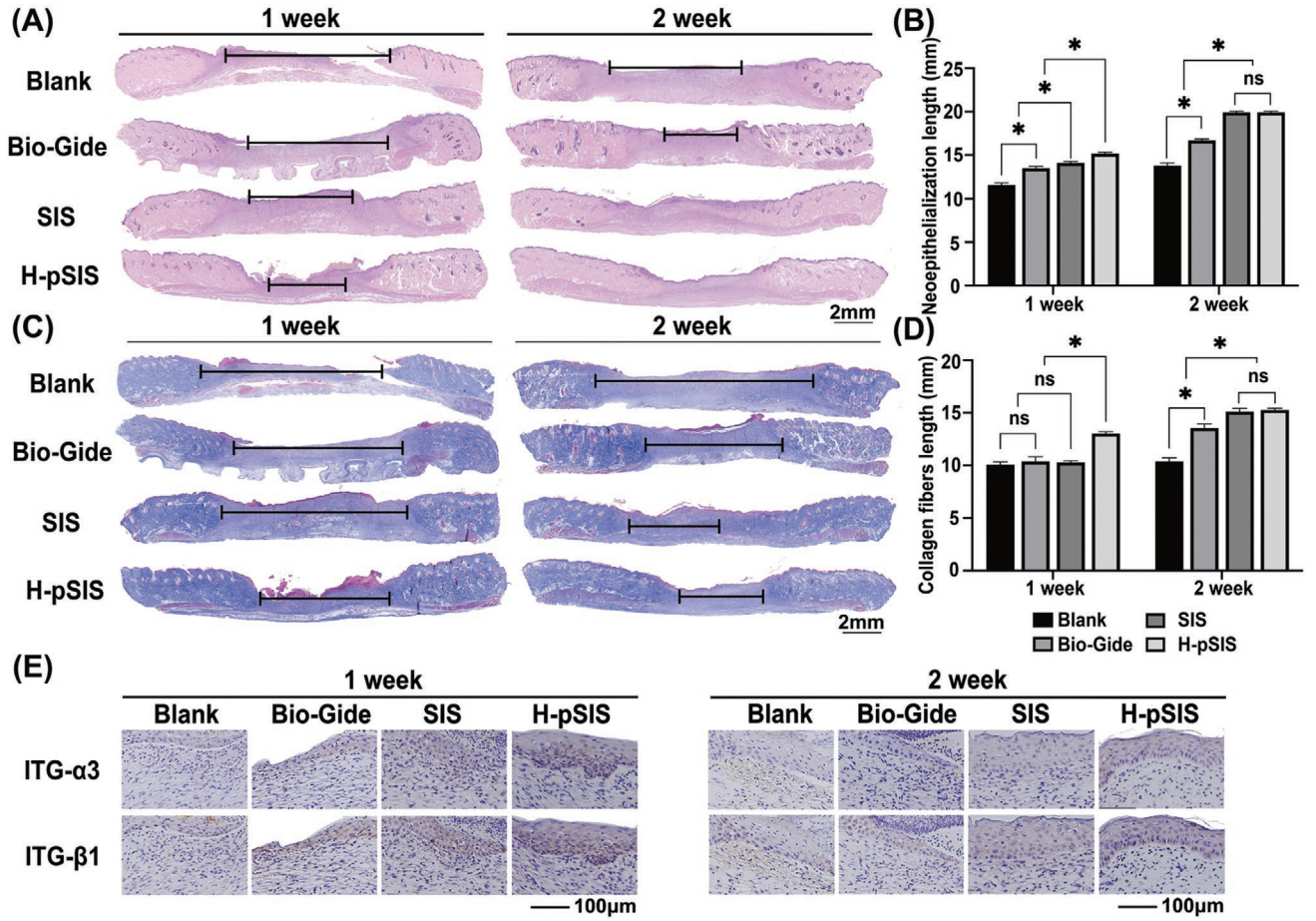

Figure 8. Evaluation of healing-promoting ability of pSIS in rat skin defect model at one and two weeks. A) H&E staining (segment: length of unepithelized wound). B) Neoepithelialization length (* represents $p < 0.05$). C) Masson's trichrome staining (segment: length of non-collagenous fiber of wound). D) Collagen fibers length (* represents $p < 0.05$). E) Immunohistochemical analysis of ITG-α3 and ITG-β1 expression.

Briefly, promoting early healing of wounds after GBR is an effective method to prevent microbial infections and biomaterial exposure complications. At present, some GBR membranes possess a certain role in guiding soft tissue healing, but have single performance and limited effects.[37] The pSIS membrane developed in this study could simultaneously exert the functions of antibacterial, promoting soft tissue healing and bone regeneration, which enriched the performance of GBR membrane greatly and might provide a prospect for the clinical treatment of infectious bone defects.

3. Conclusion

In conclusion, multifunctional modification of SIS membrane with chimeric peptides was successfully developed. A set of antibacterial, osteogenic, and healing-promoting chimeric peptides which were targeted on the surface of SIS membrane by collagen binding sequences. The pSIS promoted the expression of BMP2, RUNX2, ALP, OPN, ITG-α3, and ITG-β1 as well as inhibited the growth of *S. gordonii* and *S. sanguis*, which allowed SIS membrane to exert osteogenic, healing-promoting, and antibacterial biofunctions. This study provided experimental evidence for the development of membranes of GBR and the clinical treatment of infectious bone defects.

4. Experimental Section

Synthesis and Structure Prediction of Chimeric Peptides: Chimeric peptides were synthesized to 95% purity by Fmoc solid-phase peptide synthesis method (Jill Biochemical Shanghai Co., Ltd., China) according to the sequences in Table S1 (Supporting Information). P1, P2 were labeled with rhodamine B (RB, red) and P3, P4 were labeled with fluorescein isothiocyanate (FITC, green) for CLSM. The secondary structures were analyzed by software PSIPRED. The tertiary structures were predicted by protein analysis software Robetta and visualized by VMD.

Fabrication and Morphological Observation of Chimeric Peptide Modified SIS Membrane: The SIS membrane (Beijing Biosis Healing Biological Technology Co., Ltd., China) was cut into a circle matched with different culture plates size. The four chimeric peptides were prepared into 50, 100, 200, and 400 $\times$ 10^{-6} M solution, respectively. The SIS membrane was soaked in the first peptide solution for 10 min, then washed with phosphate buffer saline (PBS) for three times and soaked in the next peptide solution. After following this method until all four peptide solutions were soaked, the pSIS was obtained. The binding ability of chimeric peptides was investigated by CLSM (LSM900, Zeiss, Germany).

According to the results of CLSM, the SIS membranes soaked in four peptide solution concentrations of 50, 100, and 200 $\times$ 10^{-6} M were

labeled as L-pSIS, M-pSIS, and H-pSIS group. These membranes were frozen overnight and lyophilized. After sputter-coated with gold, the surface morphology of the SIS and pSIS membranes was observed by SEM (Gemini 300, Zeiss, Germany).

Release of Chimeric Peptides on the pSIS Membrane: 1×10^4 BMSCs or OECs in 1000 µL of Dulbecco's modified Eagle's medium (DMEM, Gibco, USA) with 10% fetal bovine serun (FBS, Gibco, USA) were seeded onto the 24-well plates in which the H-pSIS membranes were placed and cultured at 37 °C with 5% CO_2. After 1, 3, and 7 d of culture, the cells were fixed in 4% formaldehyde (Solarbio, China) for 10 min, then infiltrated in 0.5% Triton X-100 (Sigma-Aldrich, USA) for 5 min. After washed three times with PBS, the nucleus were stained with 5 mg mL^{-1} 4′,6-diamidino-2-phenylindole (DAPI, Solarbio, China) for 5 min. The samples were observed by CLSM.

Biocompatibility of pSIS: The BMSCs or OECs were seeded on the culture plate, SIS or pSIS. On the fourth day, the cells were collected and centrifuged to remove the supernatant. Adding CellTrace CFSE (1:1000 dilution, Thermo Fisher Scientific, USA) for staining. The cells were gently resuspended and incubated at 37 °C in the dark for 20 min. Then, the medium was added and incubated at 37 °C for 5 min. The cells were centrifuged again to remove the supernatant and resuspended with fresh, pre-warmed medium for flow cytometry analysis (BD LSRFortessa, BD, USA). The data were analyzed using FlowJo.

Using the same method to seeded BMSCs or OECs onto the 24-well plates. After 1, 2, 4, and 6 d, 100 µL CCK-8 solutions (Solarbio, China) were added to each sample. After incubated at 37 °C with 5% CO_2 for 4 h, the relative cell viability was determined by measuring the light absorbance (OD) at 450 nm.

Antibacterial Activity of pSIS In Vitro: *S. sanguis* (ATCC 10556) and *S. gordonii* (ATCC 51656) were cultured separately in brain heart infusion (BHI) agar plates for 18 h at 37 °C. Then, the bacteria were resuspended at 1×10^7 colony forming units (CFU) mL^{-1} as a primary inoculum. In a 100 mm bacterial culture dish, 20 mL BHI solution mixed with 100 µL bacterial solution was inoculated. After coagulation, the SIS, M-pSIS, and H-pSIS membranes were placed in the center, and the blank well was used as the control. After 24 h, the inhibition rings were observed and photographed.

In addition, after primary inoculum of *S. sanguis* or *S. gordonii* was inoculated and incubated on the SIS, M-pSIS, and H-pSIS membranes for 24 h, the membranes were washed with PBS three times and then stained with the Live/dead staining kit (Life Technologies Corporation, CA) on new plates. The dead bacteria (red), live bacteria (green), and Alexa Fluor 405 labeled peptides (blue) could be observed by CLSM.

Cell Migration Activity of pSIS In Vitro: SIS, M-pSIS, or H-pSIS membranes and 500 µL medium (2% FBS) were put into the lower compartment of the transwell plate, and the blank well just had medium was served as the control. Then, 1×10^4 OECs or BMSCs in 500 µL of medium (2% FBS) were seeded onto transwell inserts (Thermo Fisher Scientific, USA). After 24 h, media within the transwell inserts was removed carefully. Cells were fixed with 4% formaldehyde for 30 min, permeabilized with 0.01% Triton X-100 for 5 min and stained with 1% crystal violet (Sigma-Aldrich, USA). The cells without migration were removed by gently wiping with a cotton swab. Then, migrated cells were viewed and imaged with an inverted fluorescence microscope (Olympus IX71, Japan).

1×10^5 OECs were seeded onto six-well plates with SIS, M-pSIS, and H-pSIS membranes and cultured for 24 h. Then, scraped the cells down by a cell scraper and collected them by 1000 rpm centrifugation for 3 min. Each sample required 1×10^6 OECs. Subsequently, differentially expressed genes were commercially detected by RNA-seq (Beijing Nuohe Zhiyuan Biological Mdt InfoTech Ltd., China). Quantitative real-time polymerase chain reaction (qRT-PCR) analysis, Western blot analysis, and immunofluorescence staining were used to detect differentially expressed factors after OECs were culturing for 24 h.

Osteogenic Activity of pSIS In Vitro: The osteoinductive medium containing 10×10^{-3} M β-glycerophosphate (Sigma, USA), 100×10^{-9} M dexamethasone (Sigma, USA), and 50×10^{-6} M ascorbate (Sigma, USA) was prepared. 1×10^5 BMSCs were inoculated on SIS, M-pSIS, and H-pSIS membranes in six-well plates for culturing 3 d with culture medium, and then the osteoinductive medium was used instead. After 7, 14, and 21 d, the expression of BMP2, RUNX2, ALP, and OPN was detected.

qRT-PCR Analysis in Cell Culture: Total cellular RNA was extracted by using Trizol (Gibco, USA). cDNA was synthesized using GoScript Reverse Transcription Mix (Promega, USA). The qRT-PCR analysis was performed on the Roche LC480II system (Roche, Switzerland) using a GoTaq qPCR Master Mix (Promega, USA). The data were calculated using GAPDH as the internal control by the $^{\Delta\Delta}$Ct method. The sequences of primers are listed in Table S2 (Supporting Information).

Western Blot Analysis in Cell Culture: After culturing, proteins were separated by electrophoresis and transferred to polyvinylidene fluoride (PVDF) membranes (Sigma-Aldrich, USA). After sealing with 5% bovine serum albumin (BSA, Sigma-Aldrich, USA) at room temperature for 1 h, PVDF membranes were probed with 1:1000 primary antibodies (Abcam, UK) at 4 °C overnight. Then, they were incubated with a corresponding secondary antibody at 1:5000 dilution for 1 h at room temperature. And a Pierce ECL Western Blotting Substrate (Thermo Fisher Scientific, USA) was used to detect antibody-bound proteins. Image J software was used for quantitative analysis.

Immunofluorescence Staining in Cell Culture: 1×10^4 BMSCs or OECs were seeded onto 24-well plates cultured with 1 mL leaching solution of SIS, M-pSIS, or H-pSIS membranes and then BMSCs were cultured with osteoinductive medium. After the corresponding culture period, BMSCs or OECs were fixed in 4% formaldehyde for 30 min, permeabilized with 0.5% Triton X-100 for 5 min, and blocked in 5 mg mL^{-1} BSA solution for 1 h. Then, cells were incubated with primary antibodies (Abcam, UK) at 1:200 dilution at 37 °C for 2 h. After that, they were incubated with Cy3-conjugated anti-rabbit/mouse secondary antibody at 1:200 dilution (Abcam, UK) for 1 h and then stained with 1 mg mL^{-1} DAPI for 10 min. CLSM was used to visualize.

Osteogenic Activity of pSIS In Vivo: Animal experiments in this work were approved by the Animal Ethical Committee of the Academic Medical Center at the Tianjin Medical University. Briefly, the experiment was divided into blank control, SIS, Bio-Gide, and H-pSIS groups. The Sprague-Dawley (SD) rats (250–280 g, male, 6–8 weeks) were anesthetized by inhaling isoflurane. Then, the parietal calvarium was exposed by cutting the skin. Subsequently, a full-thickness defect with a diameter of 8 mm was made in the center of the skull with a trephine. The blank control group was not treated, the other three groups were placed with corresponding membranes on the defects. Finally, the wound was stitched up.

At the end of 12 weeks, the rats were euthanasia. The bone defects were taken out and fixed in 4% paraformaldehyde for 24 h. Then, the samples were scanned with Micro-CT (SkyScan 1276, Germany) for standardized reconstruction and evaluating new bone formation. Next, the samples were decalcified with a rapid decalcifying fluid (Rapid Cal Immuno, ZS-Bio, China) for 7 d. After being dehydrated and paraffin-embedded, the samples were sliced at 5 µm in thickness. H&E and Masson's trichrome staining (Solarbio, China) was used for histological analysis. The primary antibodies anti-OCN, anti-COL1, and fluorescence-conjugated secondary antibody IgG at 1:200 dilution (Abcam, UK) were used for immunohistochemistry. The sections were observed using a quantitative analysis system for whole landscape imaging of tissue slices (Vectra Polaris, PerkinElmer, USA).

Healing-Promoting Ability of pSIS In Vivo: The SD rats were anesthetized by inhaling isoflurane and fixed in prone position. After removing the hair of the back, four symmetrical round marks were made by using a punch (2 cm in diameter) on both sides of the spine. Along the round marks, the entire skin was cut off with a scalpel and divided into groups as follows: blank control, SIS group, Bio-Gide group, and H-pSIS group, and the membrane was sutured and fixed with subcutaneous tissue. Each rat was raised separately to avoid biting each other. One and two weeks after operation, photos were taken and skin samples were collected. Specific methods of H&E, Masson's trichrome staining, and immunohistochemistry were the same as above. The expressions of ITG-β1 and ITG-α3 were detected by immunohistochemistry.

Statistical Analysis: All experiments data were expressed as means ± standard deviations (SD) which were repeated at least three times. Statistical analysis was assessed using single factor analysis of variance (ANOVA) with Tukey's test. A *p*-value less than 0.05 was considered to have significant statistical difference (* $p < 0.05$).

Supporting Information

Supporting Information is available from the Wiley Online Library or from the author.

Acknowledgements

Y.M. and S.M. contributed equally to this work. This work was jointly supported by the National Natural Science Foundation of China (NSFC, Grant No. 81701019), the China Postdoctoral Science Foundation (Grant Nos. 2019M660270 and 2020M680253), the Scientific Foundation of Tianjin Education Commission (Grant No. 2019KJ173), and the Science and technology project of Tianjin Health Committee (Grant No. QN20026).

Conflict of Interest

The authors declare no conflict of interest.

Data Availability Statement

The data that support the findings of this study are available from the corresponding author upon reasonable request.

Keywords

antibacterial, chimeric peptides, osteogenic, SIS membrane, would healing

Received: February 9, 2021
Revised: April 3, 2021
Published online:

[1] a) E. Jimi, S. Hirata, K. Osawa, M. Terashita, C. Kitamura, H. Fukushima, *Int. J. Dent.* **2012**, *2012*, 1; b) R. E. Jung, N. Fenner, C. H. Hammerle, N. U. Zitzmann, *Clin. Oral Implants Res.* **2013**, *24*, 1065.
[2] Z. Sheikh, C. Sima, M. Glogauer, *Materials* **2015**, *8*, 2953.
[3] a) A. D. Theocharis, S. S. Skandalis, C. Gialeli, N. K. Karamanos, *Adv. Drug Delivery Rev.* **2016**, *97*, 4; b) T. Sun, S. Yao, M. Liu, Y. Yang, Y. Ji, W. Cui, Y. Qu, X. Guo, *Tissue Eng., Part A* **2018**, *24*, 502.
[4] a) Y. Ji, J. Zhou, T. Sun, K. Tang, Z. Xiong, Z. Ren, S. Yao, K. Chen, F. Yang, F. Zhu, X. Guo, *J. Biomed. Mater. Res., Part A* **2019**, *107*, 689; b) J. Hodde, *Tissue Eng.* **2002**, *8*, 295.
[5] B. Andree, A. Bar, A. Haverich, A. Hilfiker, *Tissue Eng., Part B* **2013**, *19*, 279.
[6] a) S. W. Chang, S. Y. Shin, J. R. Hong, S. M. Yang, H. M. Yoo, D. S. Park, T. S. Oh, S. B. Kye, *Oral Surg. Oral Med. Oral Pathol. Oral Radiol. Endod.* **2009**, *107*, 197; b) A. J. van Winkelhoff, *Eur. J. Oral Implantol.* **2012**, S43.
[7] L. Shi, V. Ronfard, *Int. J. Burns Trauma* **2013**, *3*, 173.
[8] R. Nordstrom, M. Malmsten, *Adv. Colloid Interface Sci.* **2017**, *242*, 17.
[9] S. Melino, C. Santone, P. Di Nardo, B. Sarkar, *FEBS J.* **2014**, *281*, 657.
[10] a) A. Jurczak, D. Koscielniak, M. Papiez, P. Vyhouskaya, W. Krzysciak, *Biol. Res.* **2015**, *48*, 61; b) T. Imatani, T. Kato, K. Minaguchi, K. Okuda, *Oral Microbiol. Immunol.* **2000**, *15*, 378.
[11] Z. Liu, S. Ma, S. Duan, D. Xuliang, Y. Sun, X. Zhang, X. Xu, B. Guan, C. Wang, M. Hu, X. Qi, X. Zhang, P. Gao, *ACS Appl. Mater. Interfaces* **2016**, *8*, 5124.
[12] S. Makihira, T. Shuto, H. Nikawa, K. Okamoto, Y. Mine, Y. Takamoto, M. Ohara, K. Tsuji, *Int. J. Mol. Sci.* **2010**, *11*, 1458.
[13] S. Makihira, H. Nikawa, T. Shuto, M. Nishimura, Y. Mine, K. Tsuji, K. Okamoto, Y. Sakai, M. Sakai, N. Imari, S. Iwata, M. Takeda, F. Suehiro, *J. Mater. Sci.: Mater. Med.* **2011**, *22*, 2765.
[14] a) I. A. van Dijk, A. F. Beker, W. Jellema, K. Nazmi, G. Wu, D. Wismeijer, P. M. Krawczyk, J. G. Bolscher, E. C. Veerman, J. Stap, *J. Dent. Res.* **2017**, *96*, 430; b) P. Torres, J. Diaz, M. Arce, P. Silva, P. Mendoza, P. Lois, A. Molina-Berrios, G. I. Owen, V. Palma, V. A. Torres, *FASEB J.* **2017**, *31*, 4946.
[15] a) M. J. Oudhoff, J. G. Bolscher, K. Nazmi, H. Kalay, W. van 't Hof, A. V. Amerongen, E. C. Veerman, *FASEB J.* **2008**, *22*, 3805; b) M. J. Oudhoff, K. L. Kroeze, K. Nazmi, P. A. van den Keijbus, W. van 't Hof, M. Fernandez-Borja, P. L. Hordijk, S. Gibbs, J. G. Bolscher, E. C. Veerman, *FASEB J.* **2009**, *23*, 3928.
[16] Z. Liu, S. Ma, X. Lu, T. Zhang, Y. Sun, W. Feng, G. Zheng, L. Sui, X. Wu, X. Zhang, P. Gao, *Chem. Eng. J.* **2019**, *356*, 117.
[17] a) J. Takagi, H. Asai, Y. Saito, *Biochemistry* **1992**, *31*, 8530; b) H. Wahyudi, A. A. Reynolds, Y. Li, S. C. Owen, S. M. Yu, *J. Controlled Release* **2016**, *240*, 323.
[18] T. M. Chiang, F. Cole, V. Woo-Rasberry, *J. Biol. Chem.* **2002**, *277*, 34896.
[19] G. Li, Z. Huang, C. Zhang, B. J. Dong, R. H. Guo, H. W. Yue, L. T. Yan, X. H. Xing, *Appl. Microbiol. Biotechnol.* **2016**, *100*, 215.
[20] P. Argos, *J. Mol. Biol.* **1990**, *211*, 943.
[21] Y. Zhang, Y. Chen, B. Zhao, J. Gao, L. Xia, F. Xing, Y. Kong, Y. Li, G. Zhang, *Regener. Biomater.* **2020**, *7*, 577.
[22] J. C. Wataha, *J. Prosthet. Dent.* **2001**, *86*, 203.
[23] a) P. E. Kolenbrander, R. J. Palmer Jr., S. Periasamy, N. S. Jakubovics, *Nat. Rev. Microbiol.* **2010**, *8*, 471; b) D. F. Kinane, P. G. Stathopoulou, P. N. Papapanou, *Nat. Rev. Dis. Primers* **2017**, *3*, 17038.
[24] a) N. S. Jakubovics, J. C. Robinson, D. S. Samarian, E. Kolderman, S. A. Yassin, D. Bettampadi, M. Bashton, A. H. Rickard, *Mol. Microbiol.* **2015**, *97*, 281; b) B. Rosan, R. J. Lamont, *Microbes Infect.* **2000**, *2*, 1599.
[25] X. Ding, S. Duan, X. Ding, R. Liu, F. Xu, *Adv. Funct. Mater.* **2018**, *28*, 1802140.
[26] a) M. Ono, C. A. Inkson, T. M. Kilts, M. F. Young, *J. Bone Miner. Res.* **2011**, *26*, 193; b) J. Sun, J. Li, C. Li, Y. Yu, *Mol. Med. Rep.* **2015**, *12*, 4230.
[27] Y. H. Xuan, B. B. Huang, H. S. Tian, L. S. Chi, Y. M. Duan, X. Wang, Z. X. Zhu, W. H. Cai, Y. T. Zhu, T. M. Wei, H. B. Ye, W. T. Cong, L. T. Jin, *PLoS One* **2014**, *9*, e108182.
[28] a) M. J. Oudhoff, P. A. van den Keijbus, K. L. Kroeze, K. Nazmi, S. Gibbs, J. G. Bolscher, E. C. Veerman, *J. Dent. Res.* **2009**, *88*, 846; b) P. Torres, M. Castro, M. Reyes, V. A. Torres, *Oral Dis.* **2018**, *24*, 1150.
[29] a) J. A. Kreidberg, *Curr. Opin. Cell Biol.* **2000**, *12*, 548; b) M. Ono, A. Masaki, A. Maeda, T. M. Kilts, E. S. Hara, T. Komori, H. Pham, T. Kuboki, M. F. Young, *Matrix Biol.* **2018**, *68*, 533.
[30] H. Jakhu, G. Gill, A. Singh, *J. Oral Biol. Craniofac. Res.* **2018**, *8*, 122.
[31] T. Kinumatsu, S. Hashimoto, T. Muramatsu, H. Sasaki, H. S. Jung, S. Yamada, M. Shimono, *J. Periodontal Res.* **2009**, *44*, 13.
[32] a) J. O. Hollinger, J. C. Kleinschmidt, *J. Craniofac. Surg.* **1990**, *1*, 60; b) G. M. Cooper, M. P. Mooney, A. K. Gosain, P. G. Campbell, J. E. Losee, J. Huard, *Plast. Reconstr. Surg.* **2010**, *125*, 1685.

[33] A. K. Schlegel, H. Mohler, F. Busch, A. Mehl, *Biomaterials* **1997**, *18*, 535.
[34] A. M. Ferreira, P. Gentile, V. Chiono, G. Ciardelli, *Acta Biomater.* **2012**, *8*, 3191.
[35] K. S. Raja, M. S. Garcia, R. R. Isseroff, *Front. Biosci.* **2007**, *12*, 2849.
[36] a) C. D. Seaborn, F. H. Nielsen, *Biol. Trace Elem. Res.* **2002**, *89*, 251; b) S. Chattopadhyay, R. T. Raines, *Biopolymers* **2014**, *101*, 821.
[37] a) E. Argintar, S. Edwards, J. Delahay, *Injury* **2011**, *42*, 730; b) A. R. Sanchez, P. J. Sheridan, L. I. Kupp, *Int. J. Oral Maxillofac. Implants* **2003**, *18*, 93.